

# Assessment of the effects of ischaemia/hypoxia on angiogenesis in rat myofascial trigger points using colour Doppler flow imaging

Fangyan Jiang<sup>Equal first author, 1</sup>, Shuangcheng Yu<sup>Equal first author, 2</sup>, Haiqing Su<sup>1</sup>, Shangyong Zhu<sup>Corresp. 3</sup>

<sup>1</sup> Department of Medical Ultrasound, the Affiliated Minzu Hospital of Guangxi Medical University, Nanning, Guangxi, China

<sup>2</sup> Department of Radiology, the Affiliated Minzu Hospital of Guangxi Medical University, Nanning, Guangxi, China

<sup>3</sup> Department of Medical Ultrasound, the First Affiliated Hospital of Guangxi Medical University, Nanning, Guangxi, China

Corresponding Author: Shangyong Zhu

Email address: zhushangyong2019@hotmail.com

**Background & Aims.** Myofascial pain syndrome (MPS) is a common non-articular disorder of the musculoskeletal system that is characterized by the presence of myofascial trigger points (MTrPs). Despite the high prevalence of MPS, its pathogenesis, which induces the onset and maintenance of MTrPs, is still not completely understood. To date, no studies have investigated the changes in the biochemical milieu caused by ischaemia/hypoxia in the MTrP regions of muscle that are proposed in the integrated hypothesis. Therefore, this study investigated whether ischaemic/hypoxic conditions participate in the formation of active MTrPs and affect angiogenesis using colour Doppler flow imaging (CDFI). **Methods.** Twenty-five Sprague-Dawley rats were randomly divided into a model group and a normal control group. A model of active MTrPs was established by a blunt strike combined with eccentric exercise. Enzyme-linked immunosorbent assays (ELISAs) were employed to detect the levels of HIF-1 $\alpha$  and VEGF. Microvessel density (MVD) was evaluated using immunohistochemistry. CDFI was applied to observe the blood flow signals in the MTrPs, which were classified into four grades based on their strengths. **Results.** Compared with the control group, the active MTrP group exhibited significantly higher HIF-1 $\alpha$  and VEGF levels and MVD values. These differences were accompanied by increased blood flow signals. In the active MTrP group, the blood flow signal grade was positively correlated with the MVD ( $P < 0.05$ ) and independently correlated with the VEGF level ( $P < 0.05$ ) but was not correlated with the expression of HIF-1 $\alpha$  ( $P > 0.05$ ). **Conclusion.** Ischaemic/hypoxic conditions may be involved in the formation of MTrPs. CDFI is useful for detection of the features of angiogenesis in or surrounding MTrPs via assessment of blood flow signals.

1 **Assessment of the effects of ischaemia/hypoxia on angiogenesis**  
2 **in rat myofascial trigger points using colour Doppler flow**  
3 **imaging**

4 Fangyan Jiang<sup>1+</sup>, Shuangcheng Yu<sup>2+</sup>, Haiqing Su<sup>1</sup>, Shangyong Zhu<sup>3\*</sup>

5 <sup>1</sup> Department of Medical Ultrasound, Affiliated Minzu Hospital of Guangxi Medical University,  
6 232 Ming Xiu Rd, 530001 Nanning, Guangxi, China;

7 <sup>2</sup> Department of Radiology, Affiliated Minzu Hospital of Guangxi Medical University, 232 Ming  
8 Xiu Rd, 530001 Nanning, Guangxi, China;

9 <sup>3</sup> Department of Medical Ultrasound, First Affiliated Hospital of Guangxi Medical University, 6  
10 Shuangyong Rd, 530021 Nanning, Guangxi, China.

11 \*Corresponding Author:

12 Shangyong Zhu

13 Email address: zhushangyong2019@hotmail.com

14 <sup>+</sup> Fangyan Jiang and Shuangcheng Yu contributed equally to this work.

15

16

17

18

19

20

21

22 **Abstract**

23 **Background & Aims.** Myofascial pain syndrome (MPS) is a common non-articular disorder of  
24 the musculoskeletal system that is characterized by the presence of myofascial trigger points  
25 (MTrPs). Despite the high prevalence of MPS, its pathogenesis, which induces the onset and  
26 maintenance of MTrPs, is still not completely understood. To date, no studies have investigated  
27 the changes in the biochemical milieu caused by ischaemia/hypoxia in the MTrP regions of  
28 muscle that are proposed in the integrated hypothesis. Therefore, this study investigated whether  
29 ischaemic/hypoxic conditions participate in the formation of active MTrPs and affect  
30 angiogenesis using colour Doppler flow imaging (CDFI).

31 **Methods.** Twenty-five Sprague-Dawley rats were randomly divided into a model group and a  
32 normal control group. A model of active MTrPs was established by a blunt strike combined with  
33 eccentric exercise. Enzyme-linked immunosorbent assays (ELISAs) were employed to detect the  
34 levels of HIF-1 $\alpha$  and VEGF. Microvessel density (MVD) was evaluated using  
35 immunohistochemistry. CDFI was applied to observe the blood flow signals in the MTrPs, which  
36 were classified into four grades based on their strengths.

37 **Results.** Compared with the control group, the active MTrP group exhibited significantly higher  
38 HIF-1 $\alpha$  and VEGF levels and MVD values. These differences were accompanied by increased  
39 blood flow signals. In the active MTrP group, the blood flow signal grade was positively  
40 correlated with the MVD ( $P < 0.05$ ) and independently correlated with the VEGF level ( $P <$   
41  $0.05$ ) but was not correlated with the expression of HIF-1 $\alpha$  ( $P > 0.05$ ).

42 **Conclusion.** Ischaemic/hypoxic conditions may be involved in the formation of MTrPs. CDFI is  
43 useful for detection of the features of angiogenesis in or surrounding MTrPs via assessment of  
44 blood flow signals.

## 45 INTRODUCTION

46 Myofascial pain syndrome (MPS) is a common non-articular disorder of the musculoskeletal  
47 system affecting as many as 15% of patients treated in general medical practice and up to 85%  
48 patients treated at pain management centres (*Fleckenstein et al., 2010; Srbely et al., 2016*). MPS  
49 is characterized by the presence of myofascial trigger points (MTrPs), which are discrete, stiff  
50 and hyperirritable nodules in taut bands of skeletal muscle that can be palpated during a physical  
51 examination (*Shah et al., 2015*). MTrPs are clinically classified as active or latent. Many  
52 physicians currently make a definite diagnosis of MPS upon finding one or more MTrPs.  
53 Knowledge of the underlying aetiology of MTrPs is critical not only for preventing their  
54 development and recurrence but also for inactivating and eliminating existing MTrPs (*Bron et*  
55 *al., 2012*). A consensus has been developed that muscle overuse, direct trauma or psychological  
56 stress lead to the development of MTrPs (*Simons et al., 1999; Shah et al., 2015*). Most  
57 individuals experience muscle pain as a result of trauma, injury, overuse, or strain at some point  
58 in their lives (*Shah et al., 2015*). If the muscle pain persists for a long period after resolution of  
59 the injury factors and if normal recovery is disrupted, MTrPs may develop.

60 Despite the high prevalence of MPS, its pathogenesis, which induces the onset and  
61 maintenance of MTrPs, is still not completely understood (*Jafri et al., 2014*). Currently, an  
62 intriguing possible mechanism mentioned by Simons, “The Integrated Trigger Point  
63 Hypothesis”, is widely accepted by various researchers and postulates that an “energy crisis”

64 perpetuates an initial, sustained, low-level muscle contraction, and a decrease in intramuscular  
65 perfusion is presumed to exist (*Simons et al., 1999*). These changes lead to local ischaemia,  
66 hypoxia, and insufficient ATP synthesis, which are responsible for increases in acidity and  $\text{Ca}^{2+}$   
67 accumulation and subsequent sarcomere contraction. When sarcomere contraction persists, local  
68 intramuscular perfusion may be decreased, and ischaemia/hypoxia can persist. This vicious cycle  
69 likely leads to the development of MTrPs (*Shah et al., 2015; Simons et al., 1999*).

70 According to previous studies, increased levels of pain and inflammatory biomarkers have  
71 been detected in the vicinity of active MTrPs (*Shah et al., 2008; Shah et al., 2005; Grosman-  
72 Rimon et al., 2016; Lv et al., 2018*). These findings objectively support Simons' integrated  
73 hypothesis. However, to date, no studies have investigated the changes in the biochemical milieu  
74 caused by ischaemia/hypoxia in the MTrP regions of muscle, and researchers have not yet  
75 clearly determined whether these changes are involved in the progression of MTrPs. Hypoxia  
76 increases the expression of HIF-1 $\alpha$ , a key oxygen concentration-dependent transcription factor,  
77 subsequently regulating the expression of its downstream target gene VEGF (*Pugh et al., 2003*).  
78 Discovery of this mechanism has confirmed that ischaemia/hypoxia regulates the process of  
79 angiogenesis (*Pugh et al., 2003*). In addition, VEGF has also been confirmed to be involved in  
80 muscle repair mechanisms and capillary formation in skeletal muscle (*Olfert et al., 2010; Li et  
81 al., 2010*). Thus, the levels of HIF-1 $\alpha$  and VEGF likely increase in response to active MTrPs.

82 In this study, an active MTrP model based on direct trauma was established in rats using a  
83 method described in a previous study (*Huang et al., 2013*). The aim of the present study was to  
84 compare the levels of HIF-1 $\alpha$ , VEGF and microvessel density (MVD) between an active MTrP  
85 group and a normal control group to confirm the occurrence of ischaemia/hypoxia, as mentioned

86 in the integrated hypothesis, and to investigate whether these indicators are associated with the  
87 grades of blood flow signals on ultrasound.

## 88 **MATERIALS AND METHODS**

### 89 **Experimental animals**

90 Twenty-five healthy male Sprague-Dawley rats that were 7 weeks old (body weight: 200–220 g)  
91 were purchased from the Animal Experiment Center of Guangxi Medical University (Nanning,  
92 China) and randomly divided into two groups: (1) a normal control group (n = 10) and (2) a  
93 model group (n = 15). All rats were housed in a pathogen-free animal facility with a controlled  
94 temperature of 22–24°C and 42% humidity and maintained on a constant 12 h dark/12 h light  
95 cycle. The animals were provided free access to food and water. At the end of the experiment, all  
96 rats were euthanized by intraperitoneal injection of pentobarbital sodium (200 mg/kg), and tissue  
97 sections were obtained. The animal experiments were conducted in accordance with local  
98 protocols for the care and use of laboratory animals. The procedures were all approved by the  
99 Animal Experiment Center of Guangxi Medical University—also known as the Animal Ethics  
100 Committee of Guangxi Medical University—approved this study (Approval No: 201904013).

### 101 **Animal model**

102 The active MTrP model was established as described by Huang et al through a blunt strike in  
103 combination with eccentric exercise for 8 weeks (*Huang et al., 2013*). Rats were anaesthetized  
104 by injection of 30 mg/kg pentobarbital sodium before being fixed on the board of a homemade  
105 striking device every Saturday. A blunt strike was administered to an area of the right proximal  
106 gastrocnemius that had been marked on the skin using a 1200 g stick freely dropped from a  
107 height of 20 cm with a kinetic energy of 2.352 J. On the second day (every Sunday), all injured

108 rats underwent 90 minutes of eccentric exercise on a treadmill (SA101B, Jiangsu Saiangsi  
109 Biological Technology Co., Ltd., Nanjing, China) at a  $-16^\circ$  downhill angle and speed of 16  
110 m/min. Subsequently, the rats rested for 5 days a week without any intervention. All rats in the  
111 model group received this treatment for 8 weeks with 4 subsequent weeks of rest, while the rats  
112 in the control group did not undergo any intervention in this period.

113

#### 114 **Ultrasound image processing**

115 After modelling, the fur and skin covering the right gastrocnemius area were shaved and cleaned.  
116 Then, all rats underwent ultrasonographic examination using an Aplio 500 clinical ultrasound  
117 (US) system (Toshiba Medical System Corporation, Tochigi, Tokyo, Japan ) with a linear array  
118 transducer (5–14 MHz). The presence of MTrPs within the taut band was determined by two  
119 diagnostic sonographers with 10 and 16 years of experience using a combination of greyscale  
120 imaging and sonoelastography. According to previous studies (*Sikdar et al., 2009; Kumbhare et*  
121 *al., 2016; Shankar et al., 2012*), MTrPs are focal hypoechoic (darker) or hyperechoic (brighter)  
122 areas with heterogeneous echotextures on greyscale images and stiffer regions on  
123 sonoelastography than the surrounding tissues. In the present study, strain elastography (SE) was  
124 applied to identify the MTrPs using real-time colour elastography and greyscale US imaging.  
125 The hardness of tissues increased gradually, as shown by colours ranging from green (soft tissue)  
126 to blue (hard tissue). Colour Doppler flow imaging (CDFI) was applied to detect blood flow in  
127 the MTrPs. The blood flow signals were semiquantitatively classified into the following four  
128 grades based on the criteria reported by Adler (*Adler et al., 1990*): grade 0, no blood flow signal;  
129 grade I, one or two dot-like blood flow signals; grade II, three dot-like or thin and short blood

130 flow signals; and grade III, one or more large and long blood flow signals (Fig. 1). When more  
131 than one MTrP was diagnosed within the gastrocnemius area using US imaging, the point with  
132 the richest blood flow signal in the referenced location was chosen.

133

#### 134 **Electromyographic and histological assays**

135 All rats were examined by electromyography (EMG) using an NTS-2000 instrument (Nuocheng  
136 Medical Co., Ltd., Shanghai). First, the right gastrocnemius area of each rat was completely  
137 exposed. The palpable taut band of muscle was marked. Then, an electrode was inserted into the  
138 taut band to detect the local twitch responses and spontaneous electrical activity (SEA), which  
139 determined the presence of active MTrPs (*Huang et al., 2013*). After the SEA was determined,  
140 segments of muscle corresponding tissue were excised and fixed in formalin buffer for  
141 subsequent assessment of the histological changes in active MTrPs. Similarly, the rats in the  
142 control group underwent EMG, and histological assays were performed at the same positions.

143

#### 144 **Microvessel density analysis**

145 Muscle slices from the two groups of rats were stained with a cluster of differentiation 31 (CD  
146 31) antibody to quantify the MVD (number of vessels). Paraffin sections were fixed and stained  
147 with haematoxylin-eosin (HE). The primary anti-CD31 antibody (1: 500, v/v) was added, and the  
148 sections were incubated overnight at 4°C. After three 5-minute washes, the sections were  
149 incubated with a secondary anti-mouse IgG (1:2000) antibody at 37°C for 1 h. Then, the samples  
150 were washed with PBS. The area with the highest microvascular numbers (hot spot) was selected

151 under a  $\times 40$  optical field of view in three different fields as described by Weidner (*Weidner et*  
152 *al., 1991*). The average number of microvessels in the three selected fields at  $\times 200$  magnification  
153 was calculated.

154

### 155 **Enzyme-linked immunosorbent assay**

156 Due to the extremely small sizes of MTrPs ( $3\text{--}4\text{ mm}^2$ ), homogenates were prepared from muscle  
157 tissue in the vicinity of MTrPs to increase the sensitivity of the test. The tissue samples were cut,  
158 weighed, frozen in liquid nitrogen and stored at  $-80^\circ\text{C}$ . Muscle tissue (100 mg) was rinsed with  
159  $1\times$  PBS, homogenized in 1 ml of  $1\times$  PBS and stored overnight at  $-20^\circ\text{C}$ . After two freeze-thaw  
160 cycles were performed to disrupt the cell membranes, the homogenates were centrifuged at 5000  
161  $\times g$  for 5 minutes at  $2\text{--}8^\circ\text{C}$ . The supernatant was removed and assayed immediately. The levels  
162 of HIF-1 $\alpha$  and VEGF were measured by enzyme-linked immunosorbent assay (ELISA)  
163 according to the manufacturer's instructions (Cusabio Biotech Co., Ltd., Wuhan, China).

164

### 165 **Statistical analysis**

166 All data were analysed with SPSS 22.0 software (Chicago, IL, USA). The normality of the data  
167 was assessed using the Kolmogorov-Smirnov test. Descriptive statistics, including the HIF-1 $\alpha$   
168 and VEGF levels and the MVD values, are presented as the means and standard deviations.  
169 Independent-sample T tests were performed to verify the differences between the MTrP group  
170 and the normal control group. The correlations between the blood flow signal grades and the

171 MVD values, VEGF levels and HIF-1 $\alpha$  levels were determined by calculating the Spearman rank  
172 correlation coefficients. For all tests used, statistical significance was set at a value of  $P < 0.05$ .

## 173 RESULTS

174 Of the 15 model rats, one died unexpectedly due to complications of anaesthesia. Therefore,  
175 24 rats survived in the present study (model group:  $n = 14$ , normal group:  $n = 10$ ).

176

### 177 Ultrasound findings

178 Via B-mode imaging, MTrPs were visualized in all rats of the model group within the taut band  
179 of the right gastrocnemius muscle in an area consistent with the location of the palpable nodule  
180 identified during physical examination. No MTrPs were observed in the control group. The great  
181 majority of MTrPs showed an ellipsoidal focal hypoechoic region, and 2 rats exhibited a  
182 hyperechoic region. Among the animals, 4 rats presented with more than one hypoechoic region,  
183 and the point of the greatest blood flow signal was chosen. The average MTrP size was  $3.3 \pm 0.18$   
184  $\text{mm}^2$ . In addition, SE imaging consistently detected a stiff focal region that was entirely covered  
185 in blue or was mostly blue with little green, which are consistent with the results described in a  
186 previous study (*Kumbhare et al., 2016*) (Fig. 2).

187 Based on the CDFI examination, the vessels in and around MTrPs exhibited higher blood  
188 flow than corresponding normal muscle sites, the latter of which showed no blood flow signals.  
189 A detailed description of the data obtained from the rats in the MTrP group is provided in Table  
190 1.

191

## 192 **Electromyography results and pathological features**

193 The taut bands of the muscles exhibiting abnormal changes on ultrasound were verified to show  
194 spontaneous electrical activity and local twitch responses using an electromyographic device.

195 The rats in the normal control group showed no electromyographic activity (Fig. 3).

196 Examination of the pathological sections of MTrP areas revealed variations in the shapes and  
197 sizes of the muscle fibres. Specifically, muscle fibres became thinner at both ends and swelled in  
198 the middle. Contraction nodules were present in the longitudinal section along with local  
199 widening of the muscle fibre gaps. However, the sizes and shapes of muscle fibres from normal  
200 controls were uniform (Fig. 4). These findings are consistent with results reported in the  
201 published literature (*Zhang et al., 2017*).

## 202 **Microvessel density detection**

203 As shown in Fig. 5, the cytoplasm of vascular endothelial cells in the gastrocnemius muscles of  
204 rats was stained brownish-yellow with an antibody against the CD31 protein. The MVDs of the  
205 model and control groups observed under  $\times 200$  optical magnification were  $123.64 \pm 9.56$  and  
206  $84.70 \pm 13.46$ , respectively. The MVD of the MTrP group was significantly higher than that of the  
207 control group ( $P = 0.000$ ). Additionally, comparison of the vascular morphology of the two  
208 groups revealed that the blood vessels in the MTrP group were thicker and less regularly  
209 distributed than the vessels in the control group.

210

## 211 **HIF-1 $\alpha$ and VEGF expression in the two groups**

212 HIF-1 $\alpha$  and VEGF levels were measured in muscle tissue homogenates from the two groups of  
213 rats. As shown in Fig. 6, significantly higher levels of HIF-1 $\alpha$  and VEGF were detected in the  
214 MTrP group than in the normal control group ( $P < 0.05$ ).

215

### 216 **Analysis of correlations between blood flow signals and HIF-1 $\alpha$ levels, VEGF levels and** 217 **microvessel densities in the myofascial trigger point group**

218 In the active MTrP group, linear correlation analysis were performed between VEGF levels and  
219 MVDs and the blood flow signal grades. The correlation coefficients were 0.595 and 0.707,  
220 respectively. A significant correlation between HIF-1 $\alpha$  levels and blood flow signal grades was  
221 not observed (Fig. 7).

## 222 **DISCUSSION**

223 The present study was conducted to determine whether ischaemia/hypoxia is involved in the  
224 formation of MTrPs, as proposed in the integrated hypothesis, and to investigate the underlying  
225 effect on angiogenesis. In the present study, an active MTrP rat model was successfully  
226 established by blunt-force trauma in combination with eccentric exercise, as confirmed through  
227 palpation of taut bands of muscle, SEA and a local twitch response according to the modified  
228 criteria defined by Travell and Simons (*Simons et al., 1999*) and consistent with the  
229 histopathological and ultrasonographic changes reported in previous studies (*Zhang et al., 2017*;  
230 *Sikdar et al., 2009*; *Kumbhare et al., 2016*; *Shankar et al., 2012*). The preliminary findings of  
231 this study were as follows: (1) significantly higher HIF-1 $\alpha$  and VEGF levels and higher MVDs  
232 were observed in rats with active MTrPs than in normal controls, and (2) blood flow signal grade  
233 detected using CDFI was positively correlated with VEGF expression and MVD. These results

234 are consistent with the intramuscular changes associated with an ischaemia-induced  
235 inflammatory microenvironment, providing objective evidence supporting the integrated  
236 hypothesis of MTrPs.

237 Simons' integrated hypothesis postulates that initial sustained low-level sarcomere  
238 contraction shapes local hypercontractions and compresses capillaries to cause local  
239 ischaemia/hypoxia, which is accompanied by increased local metabolic demands and leads to an  
240 energy crisis. This crisis contributes to the formation of MTrPs (*Simons et al., 1999*). In the  
241 presence of local ischaemia/hypoxia, tissue damage, or both, the biochemical milieu surrounding  
242 MTrPs becomes increasingly complex. Elevated levels of local biomarkers associated with pain  
243 and inflammation, including inflammatory mediators, neuropeptides, catecholamines, and  
244 cytokines, have been detected in the vicinity of active MTrPs compared with latent MTrPs or  
245 non-MTrP areas (*Shah et al. 2005; Shah et al. 2008*). Muscle pain may be associated with  
246 ischaemia-induced inflammation in taut bands (*Gerwin et al. 2001*). Furthermore, a recent study  
247 reported higher serum levels of inflammatory and anti-inflammatory biomarkers, as well as the  
248 growth factors fibroblast growth factor-2 (FGF-2), platelet-derived growth factor (PDGF), and  
249 VEGF, in an MPS group compared with a non-MPS control group (*Grosman-Rimon et al. 2016*).  
250 Thus, MTrPs may represent an ischaemia-induced inflammatory microenvironment.

251 In the present study, higher levels of HIF-1 $\alpha$  and VEGF were detected in the active MTrP  
252 group than in the normal control group. This finding indicates that ischaemia/hypoxia is involved  
253 in the formation of active MTrPs. HIF-1 $\alpha$  is a major regulator of basic adaptive responses to  
254 hypoxia (*Pugh et al., 2003*). HIF- $\alpha$  is generally present at low levels in normoxic rodent tissues  
255 and may not be detectable even in areas of physiological hypoxia (*Pugh et al., 2003;*  
256 *Rosenberger et al., 2002*). When systemic hypoxia occurs or when tissue ischaemia increases,

257 HIF- $\alpha$  expression and transcriptional activity increase. Hypoxia-inducible factors orchestrate the  
258 adaptive responses of endothelial cells to changes in oxygen tension by controlling survival,  
259 metabolism, and angiogenesis (*Potente et al., 2011*). Metabolic regulators control vessel growth  
260 by stimulating angiogenesis under hypoxic conditions to prepare tissues for oxidative  
261 metabolism (*Potente et al., 2011*). HIF- $\alpha$  subsequently regulates the expression of its  
262 downstream target gene VEGF (*Pugh et al., 2003*). VEGF, a major mediator of pathological  
263 angiogenesis with a predominant role in both tumour-induced and inflammation-induced  
264 angiogenesis (*Ferrara et al., 1996; Carmeliet et al., 2000*), directly regulates blood vessel  
265 formation (*Potente et al., 2011*). VEGF also participates in skeletal muscle injury and repair  
266 processes by increasing capillary formation in skeletal muscle and restoring blood flow to injured  
267 tissue, increasing the efficiency of skeletal muscle repair (*Olfert et al., 2010; Best et al., 2013*).  
268 In addition, the immunohistochemical staining conducted in the present study revealed an  
269 obvious increase in the MVD in the active MTrP group compared with the normal control group,  
270 directly confirming that angiogenesis was induced in zones of active MTrPs.

271       Currently, there is not a consensus in the literature regarding tissue perfusion in MTrPs.  
272 Although ischaemia/hypoxia may be an important factor contributing to trigger point formation,  
273 the associated microvascular changes have yet to be thoroughly elucidated. Previous studies  
274 seeking to describe blood vessels in MTrPs have focused mainly on the initiation of MTrPs  
275 induced by hypercontraction-mediated compression of capillary/venous beds. Studies on the  
276 microvascular changes to enable maintenance of MTrPs have not been performed. MPS is a  
277 chronic inflammatory disorder, and MTrPs are clinically classified as active or latent. Patients  
278 are considered to have active MTrPs if they have consistently experienced pain within the last 3  
279 months. During this period, prolonged ischaemia/hypoxia causes vessels to adjust their shapes

280 and functions to meet the changing oxygen demands of the tissue (*Potente et al., 2011*). In  
281 addition, it might stimulate the release of bradykinins, cytokines, substance P and inflammatory  
282 biomarkers in the muscle. The processes of chronic inflammation and angiogenesis are  
283 intimately linked and occur together (*Costa et al., 2007*). Hypoxia is a common stimulus of both  
284 processes and results in increased production of growth factors (*Carmeliet et al., 2005*;  
285 *Yancopoulos et al. 2000*). Upregulation of the transcription factor in response to blood flow  
286 ensures remodelling of the vasculature to adapt the vascular pattern to local tissue needs (*Potente*  
287 *et al., 2011*). Therefore, a logical hypothesis is that angiogenesis is increased in areas of active  
288 MTrPs compared with normal control areas.

289       Interestingly, this preliminary study confirmed an increase in the number of blood vessels  
290 and the presence of enlarged blood vessels in or around active MTrPs compared with normal  
291 muscle sites, consistent with previous reports (*Sikdar et al., 2010*; *Ballyns et al., 2011*;  
292 *Grosman-Rimon et al., 2016*). These findings may provide additional insights that will help  
293 researchers elucidate the pathophysiological mechanisms underlying the development of MTrPs.  
294 By analysing the changes in microvessel numbers, vascular morphology, and blood flow signals  
295 in the zones of MTrPs, we identified two intriguing phenomena: an increased vascular volume  
296 and an increased number of angiogenic vessels. Increased vascular volume has been observed  
297 using lumped-parameter compartment models of the skeletal circulation (*Sikdar et al., 2010*). In  
298 the current study, our observations of more microvessels, thicker blood vessels, and richer blood  
299 flow signals in MTrPs than in normal tissues confirmed the increased vascular volume in MTrP  
300 tissues compared with non-MTrP control tissues. Furthermore, the MVDs determined in the  
301 present study intuitively revealed increased numbers of angiogenic vessels. However, when  
302 analysing pathological angiogenesis, researchers should focus on the functional qualities of

303 vessels and their effects on local metabolism rather than on vessel quantity alone (*Potente et al.,*  
304 *2011*). Such information would be helpful in explaining the differences between MVD and local  
305 ischaemia in the areas of trigger points, which deserves further exploration.

306 Although the diagnosis of MTrPs was determined using conventional US combined with an  
307 SE examination, the aim of this study was to investigate the features of blood flow signals. To  
308 date, a few groups (*Sikdar et al., 2009; Sikdar et al., 2010; Ballyns et al., 2011*) have used  
309 Doppler imaging to examine the vasculature of regions surrounding MTrPs, and highly resistive  
310 vascular beds have been observed in and around the MTrPs. However, no studies have assessed  
311 the characteristics of angiogenesis at trigger points. CDFI is the most common tool used to  
312 sensitively visualize blood flow. In the present study, stronger blood flow signals were observed  
313 in the MTrP group than in the control group. In addition, conspicuous blood vessels were  
314 observed at 12 of the 14 sites in the MTrPs group, while no blood flow signals were detected in  
315 the control group. Intriguingly, the blood flow signals in the zones of MTrPs were mainly of  
316 grades I-II (9/14), with 3 cases of grade III, suggesting that the majority of subjects presented  
317 dot-like or short blood flow signals. Only two animals exhibited large and long blood vessels that  
318 passed through the trigger points, consistent with previous reports (*Sikdar et al., 2010*).

319 In addition, the blood flow signal grade was positively correlated with the VEGF level and  
320 MVD in the active MTrP group. The correlation with the VEGF level was weaker than the  
321 correlation with the MVD. Three explanations for this weak correlation are proposed. First, the  
322 MVD not only is a standard indicator of the number of angiogenesis events but also intuitively  
323 reflects the morphology and distribution of microvessels (*Magnon et al., 2007*). The  
324 neovascularization of MTrPs was greater than that of normal muscle tissue in the present study.  
325 In addition, blood vessel formation and expansion and irregular blood vessel distribution were

326 observed in the active MTrPs. The pattern obviously differed from the uniform and regular  
327 distribution of blood vessels in the control tissues. Second, VEGF is only one factor that  
328 promotes angiogenesis; other growth factors, such as FGF-2 and PDGF, are also involved  
329 (*Grosman-Rimon, 2016*). VEGF expression generally correlates closely with MVD (*Zou et al.,*  
330 *2016; Maria et al., 2005*). Third, time may elapse between VEGF expression in MTrPs and  
331 subsequent blood vessel formation that is detectable using CDFI.

332 There were some limitations of the present study. First, we adopted a tissue homogenization  
333 method to measure the levels of HIF- $\alpha$  and VEGF with ELISA to increase the sensitivity of the  
334 test, which might affect the detection of the levels of the target proteins. The serum levels were  
335 not investigated to compare with the current results. Second, both hypoechoic and hyperechoic  
336 MTrP regions were visualized using ultrasonography in the current study. The differences in the  
337 echogenicity of the MTrP regions on ultrasonography suggest differences in local tissue density  
338 features. The current study did not determine an association between a unique echo pattern and a  
339 specific MTrP histopathology. Identification of MTrPs using US imaging must be substantially  
340 improved.

## 341 CONCLUSIONS

342 As shown in the present study, significantly higher HIF-1 $\alpha$  and VEGF levels and MVDs were  
343 observed in the active MTrP group than in the normal control group, indicating that these factors  
344 may be affected by muscle ischaemia/hypoxia. These findings support the hypothesis that  
345 ischaemia/hypoxia is involved in the formation of MTrPs. In addition, the blood flow signal  
346 grade was positively correlated with the VEGF level and MVD in the active MTrP group,

347 suggesting that CDFI can be used to detect the features of angiogenesis in or surrounding MTrPs  
348 by assessing the blood flow signals.

349

350

351

## 352 **Acknowledgements**

353 The authors thank the Animal Experiment Center of Guangxi Medical University for the animal  
354 rooms and technical assistance.

355

356

## 357 **REFERENCES**

358 **Fleckenstein J, Zaps D, Ruger LJ, Lehmeier L, Freiberg F, Lang PM, Irnich D. 2010.**

359 Discrepancy between prevalence and perceived effectiveness of treatment methods in

360 myofascial pain syndrome: results of a cross-sectional, nationwide survey. BMC

361 Musculoskelet Disord **11**;11:32 DOI [10.1186/1471-2474-11-32](https://doi.org/10.1186/1471-2474-11-32).

362 **Srbely JZ, Kumbhare D, Grosman-Rimon L.2016.** A narrative review of new trends in the

363 diagnosis of myofascial trigger points: diagnostic ultrasound imaging and biomarkers. J Can

364 Chiropr Assoc **60(3)**:220-225 Available at: <https://pubmed.ncbi.nlm.nih.gov/27713577/>

- 365 **Shah JP, Thaker N, Heimur J, Aredo JV, Sikdar S, Gerber L. 2015.** Myofascial Trigger  
366 Points Then and Now: A Historical and Scientific Perspective. *PM R*7(7):746-761  
367 [DOI 10.1016/j.pmrj.2015.01.024](https://doi.org/10.1016/j.pmrj.2015.01.024).
- 368 **Bron C, Dommerholt JD. 2012.** Etiology of Myofascial Trigger Points. *Current Pain and*  
369 *Headache Reports* 16:439–444 [DOI 10.1007/s11916-012-0289-4](https://doi.org/10.1007/s11916-012-0289-4).
- 370 **Simons DG, Travell JG, Simons LS. 1999.** Travell and Simons' myofascial pain and  
371 dysfunction: the trigger point manual. Volume 1: upper half of body, 2<sup>nd</sup> ed. Baltimore:  
372 Williams Wilkins 71-72. [DOI 10.1097/00008506-200101000-00026](https://doi.org/10.1097/00008506-200101000-00026).
- 373 **Jafri SM. 2014.** Mechanisms of Myofascial Pain. *International Scholarly Research Notices*.  
374 [DOI 10.1155/2014/523924](https://doi.org/10.1155/2014/523924).
- 375 **Shah JP, Danoff JV, Desai MJ, Parikh S, Nakamura LK, Phillips TM, Gerber LH. 2008.**  
376 Biochemicals associated with pain and inflammation are elevated in sites near to and remote  
377 from active myofascial trigger points. *Arch Phys Med Rehabil* 89:16–23  
378 [DOI 10.1016/j.apmr.2007.10.018](https://doi.org/10.1016/j.apmr.2007.10.018).
- 379 **Shah JP, Phillips TM, Danoff JV, Gerber LH. 2005.** An in vivo microanalytical technique for  
380 measuring the local biochemical milieu of human skeletal muscle. *J Appl Physiol*  
381 (Bethesda, Md: 1985) 99:1977–84 [DOI 10.1152/jappphysiol.00419.2005](https://doi.org/10.1152/jappphysiol.00419.2005).
- 382 **Grosman-Rimon L, Parkinson W, Upadhye S, Clarke H, Katz J, Flannery J, Peng**  
383 **P, Kumbhare D. 2016.** Circulating biomarkers in acute myofascial pain: A case-control  
384 study. *Medicine* 95 (37):e4650 [DOI 10.1097/MD.0000000000004650](https://doi.org/10.1097/MD.0000000000004650).

- 385 **Lv H, Li Z, Hu T, Wang Y, Wu J, Li Y. 2018.** The shear wave elastic modulus and the  
386 increased nuclear factor kappa B (NF- $\kappa$ B/p65) and cyclooxygenase-2 (COX-2) expression  
387 in the area of myofascial trigger points activated in a rat model by blunt trauma to the  
388 vastus medialis. *J Biomech* **3**;66:44-50 DOI [10.1016/j.jbiomech.2017.10.028](https://doi.org/10.1016/j.jbiomech.2017.10.028).
- 389 **Pugh CW, Ratcliffe PJ. 2003.** Regulation of angiogenesis by hypoxia: Role of the HIF system.  
390 *Nat Med* **9**: 677-684 DOI [10.1038/nm0603-677](https://doi.org/10.1038/nm0603-677).
- 391 **Olfert IM, Howlett RA, Wagner PD, Breen EC. 2010.** Myocyte vascular endothelial growth  
392 factor is required for exercise-induced skeletal muscle angiogenesis. *Am J Physiol Regul*  
393 *Integr Comp Physiol* **299**:R1059–67 DOI [10.1152/ajpregu.00347.2010](https://doi.org/10.1152/ajpregu.00347.2010).
- 394 **Li J, Wei Y, Liu K, Yuan C, Tang YJ, Quan QL, Chen P, Wang W, Hu HZ, Yang L. 2010.**  
395 Synergistic effects of FGF-2 and PDGF-BB on angiogenesis and muscle regeneration in  
396 rabbit hindlimb ischemia model. *Microvasc Res* **80**:10–7 DOI [10.1016/j.mvr.2009.12.002](https://doi.org/10.1016/j.mvr.2009.12.002).
- 397 **Huang Q, Ye G, Zhao Z, Lv J, Tang L. 2013.** Myoelectrical activity and muscle morphology  
398 in a rat model of myofascial trigger points induced by blunt trauma to the vastus medialis.  
399 *Acupunct Med* **31**, 65–73 DOI [10.1136/acupmed-2012-010129](https://doi.org/10.1136/acupmed-2012-010129).
- 400 **Sikdar S, Shah JP, Gebreab T, Yen RH, Gilliams E, Danoff J, Gerber LH. 2009.** Novel  
401 Applications of ultrasound technology to visualize and characterize myofascial trigger  
402 points and surrounding soft tissue. *Arch Phys Med Rehabil* **90**:1829-38  
403 DOI [10.1016/j.apmr.2009.04.015](https://doi.org/10.1016/j.apmr.2009.04.015).
- 404 **Kumbhare DA, Elzibak AH, Noseworthy MD. 2016.** Assessment of Myofascial Trigger Points  
405 Using Ultrasound. *Am J Phys Med Rehabil* **95**(1):72-80

406 [DOI 10.1097/PHM.0000000000000376](https://doi.org/10.1097/PHM.0000000000000376).

407 **Shankar H, Reddy S. 2012.** Two- and three-dimensional ultrasound imaging to facilitate  
408 detection and targeting of taut bands in myofascial pain syndrome. *Pain Med* **13**:971- 5

409 [DOI 10.1111/j.1526-4637.2012.01411.x](https://doi.org/10.1111/j.1526-4637.2012.01411.x).

410 **Adler DD, Carson PL, Rubin JM, Quinn-Reid D. 1990.** Doppler ultrasound color flow  
411 imaging in the study of breast cancer; Preliminary findings. *Ultrasound Med Biol* **16**:553-  
412 559 [DOI 10.1016/0301-5629\(90\)90020-d](https://doi.org/10.1016/0301-5629(90)90020-d).

413 **Weidner N, Semple JP, Welch WR, Folkman J. 1991.** Tumor angiogenesis and metastasis-  
414 correlation in invasive breast carcinoma. *N Engl J Med* **324**:1-8

415 [DOI 10.1056/NEJM199101033240101](https://doi.org/10.1056/NEJM199101033240101).

416 **Zhang H, Lü J, Huang Q, Liu L, Liu Q, Eric O. 2017.** Histopathological nature of myofascial  
417 trigger points at different stages of recovery from injury in a rat model. *Acupunct Med*  
418 **35(6)**:445-451 [DOI 10.1136/acupmed-2016-011212](https://doi.org/10.1136/acupmed-2016-011212).

419 **Gerwin RD. 2001.** Classification, epidemiology, and natural history of myofascial pain  
420 syndrome. *Curr Pain Headache Rep* **5**:412–20 [DOI 10.1007/s11916-001-0052-8](https://doi.org/10.1007/s11916-001-0052-8).

421 **Rosenberger, C, Mandriota S, Jürgensen JS, Wiesener MS, Hörstrup JH, Frei  
422 U, Ratcliffe PJ, Maxwell PH, Bachmann S, Eckardt KU. 2002.** Expression of hypoxia-  
423 inducible factor-1 $\alpha$  and -2 $\alpha$  in hypoxic and ischemic rat kidneys. *J. Am. Soc. Nephrol* **13**:  
424 1721–1732 [DOI 10.1097/01.asn.0000017223.49823.2a](https://doi.org/10.1097/01.asn.0000017223.49823.2a).

425 **Potente M, Gerhardt H, Carmeliet P. 2011.** Basic and therapeutic aspects of angiogenesis.

- 426 Cell **16**;146 (6):873-87 DOI [10.1016/j.cell.2011.08.039](https://doi.org/10.1016/j.cell.2011.08.039).
- 427 **Ferrara N, Carver-Moore K, Chen H, Dowd M, Lu L, O'Shea KS, Powell-Braxton L,**  
428 **Hillan KJ, Moore MW. 1996.** Heterozygous embryonic lethality induced by targeted  
429 inactivation of the VEGF gene. *Nature* **4**;380(6573):439-42 DOI [10.1038/380439a0](https://doi.org/10.1038/380439a0).
- 430 **Carmeliet P, Jain RK. 2000.** Angiogenesis in cancer and other diseases. *Nature*  
431 **14**;407(6801):249-57 DOI [10.1038/35025220](https://doi.org/10.1038/35025220).
- 432 **Olfert IM, Howlett RA, Wagner PD, Breen EC. 2010.** Myocyte vascular endothelial  
433 growth factor is required for exercise-induced skeletal muscle angiogenesis. *Am J Physiol*  
434 *Regul Integr Comp Physiol* **299**(4):R1059–67 DOI [10.1152/ajpregu.00347.2010](https://doi.org/10.1152/ajpregu.00347.2010).
- 435 **Best TM, Gharaibeh B, Huard J. 2013.** Stem cells, angiogenesis and muscle healing: a  
436 potential role in massage therapies? *Br J Sports Med* **47**(9):556-60  
437 DOI [10.1136/bjsports-2012-091685](https://doi.org/10.1136/bjsports-2012-091685).
- 438 **Costa C, Incio J, Soares R. 2007.** Angiogenesis and chronic inflammation: cause or consequence?  
439 *Angiogenesis* **10** (3):149-66 DOI [10.1007/s10456-007-9074-0](https://doi.org/10.1007/s10456-007-9074-0).
- 440 **Carmeliet P. 2005.** Angiogenesis in life, disease and medicine. *Nature* **15**;438 (7070):932-6 DOI  
441 [10.1038/nature04478](https://doi.org/10.1038/nature04478).
- 442 **Yancopoulos GD, Davis S, Gale NW, Rudge JS, Wiegand SJ, Holash J. 2000.**  
443 Vascularspecific growth factors and blood vessel formation. *Nature* **14**:407; (6801):242-8  
444 DOI [10.1038/35025215](https://doi.org/10.1038/35025215).

- 445 **Ballyns JJ, Shah JP, Hammond J, Gebreab T, Gerber LH, Sikdar S. 2011.** Objective  
446 sonographic measures for characterizing myofascial trigger points associated with cervical  
447 pain. *J Ultrasound Med* **30** (10) : 133 1- 1340 DOI [10.7863/jum.2011.30.10.1331](https://doi.org/10.7863/jum.2011.30.10.1331).
- 448 **Sikdar S, Ortiz R, Gabreab T, Gerber LH, Shah JP. 2010.** Understanding the vascular  
449 environment of myofascial trigger points using ultrasonic imaging and computational  
450 modeling. *Conf Proc IEEE Eng Med Biol Soc* 5302-5  
451 DOI [10.1109/IEMBS.2010.5626326](https://doi.org/10.1109/IEMBS.2010.5626326).
- 452 **Magnon C, Galaup A, Rouffiac V, Opolon P, Connault E, Rosé M, Perricaudet M, Roche**  
453 **A, Germain S, Griscelli F, Lassau N. 2007.** Dynamic assessment of antiangiogenic  
454 therapy by monitoring both tumoral vascularization and tissue degeneration. *Gene Ther*  
455 **14**:108-117 DOI [10.1038/sj.gt.3302849](https://doi.org/10.1038/sj.gt.3302849).
- 456 **Zou L, Zhang G, Liu L, Chen C, Cao X, Cai J. 2016.** Relationship between PI3K pathway and  
457 angiogenesis in CIA rat synovium. *Am J Transl Res* **8** (7):3141-7 Available at:  
458 <https://www.ncbi.nlm.nih.gov/pmc/articles/PMC4969451/>
- 459 **Maria RR, Francesca C, Francesca G, Alessandro V, Gianni A, Gianna B, Vieri B, Gian**  
460 **LT. 2005.** Microdensity vessels and with vascular endothelial growth factor expression in  
461 ovarian carcinoma. *Int J Surg Pathol* **13**:135-142 DOI [10.1177/106689690501300202](https://doi.org/10.1177/106689690501300202).

## Figure 1

Description of different grades of blood flow signals in the MTrPs observed using colour Doppler flow imaging.

(A) Grade 0, no blood flow signals; (B) grade I, one or two dot-like blood flow signals; (C) grade II, three dot-like or thin and short blood flow signals; and (D) grade III, one or more large and long blood flow signals.

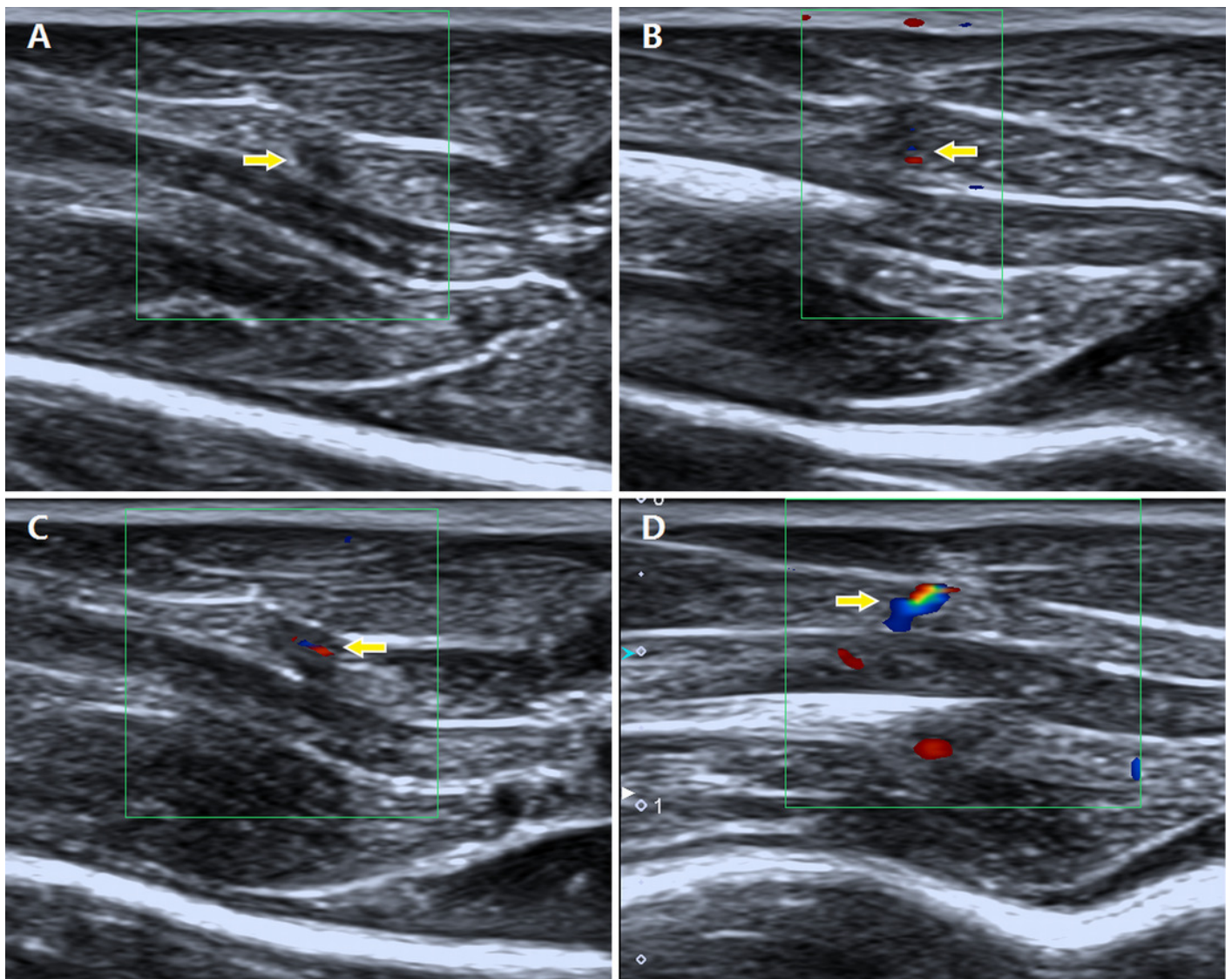


## Figure 2

Screenshot of the sonoelastography modes.

Strain elastography detection of a stiff focal region: the images presented in (A) and (B) are entirely covered in blue or are mostly blue with little green compared to the adjacent normal muscle tissue.

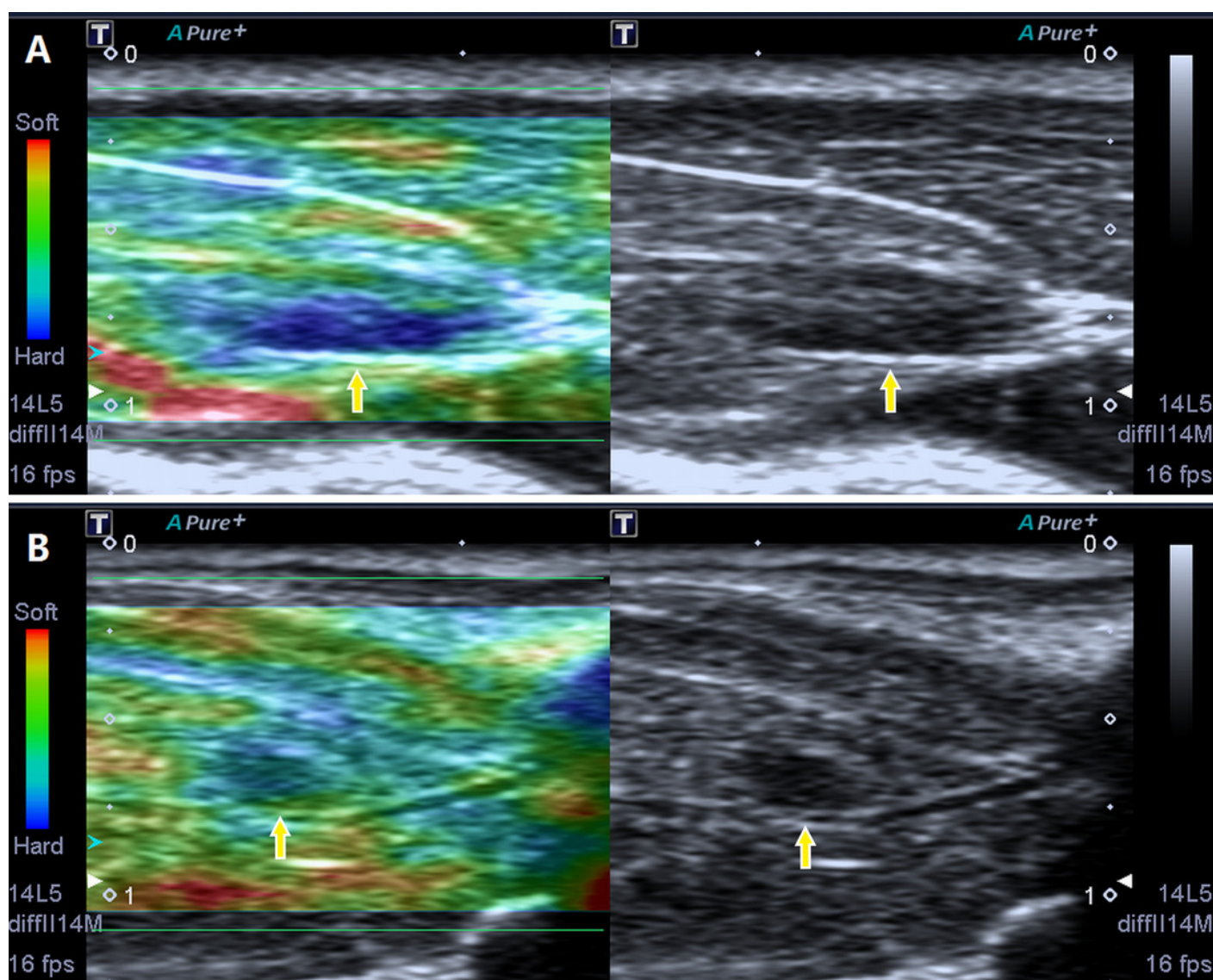


## Figure 3

EMG recordings from the two groups.

(A) muscle fibres from MTRPs presenting with spontaneous electrical activities and (B) muscle fibres from normal controls showing no EMG activity.

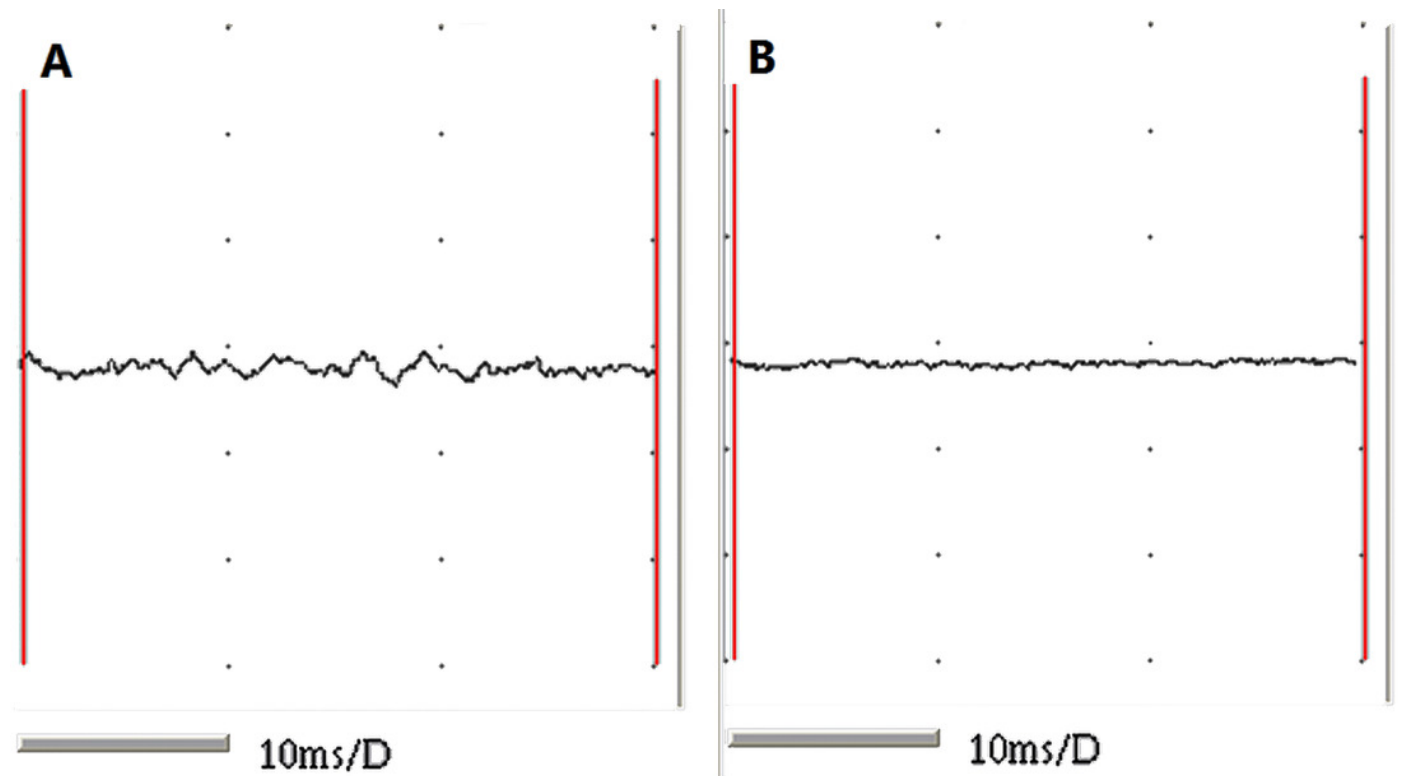


## Figure 4

Microscopic views of HE staining of muscle fibres from the two groups of rats (400×).

The histological changes in MTrPs are depicted in (A) (cross-section) and (B) (longitudinal section), and show that muscle fibres became thinner at both ends and swelled in the middle to show the contraction nodules in longitudinal sections, along with local widening of the muscle fibre gap. The histologically normal muscle fibres are similarly shown in (C) and (D), which reveal a uniform size and shape of muscle fibres.

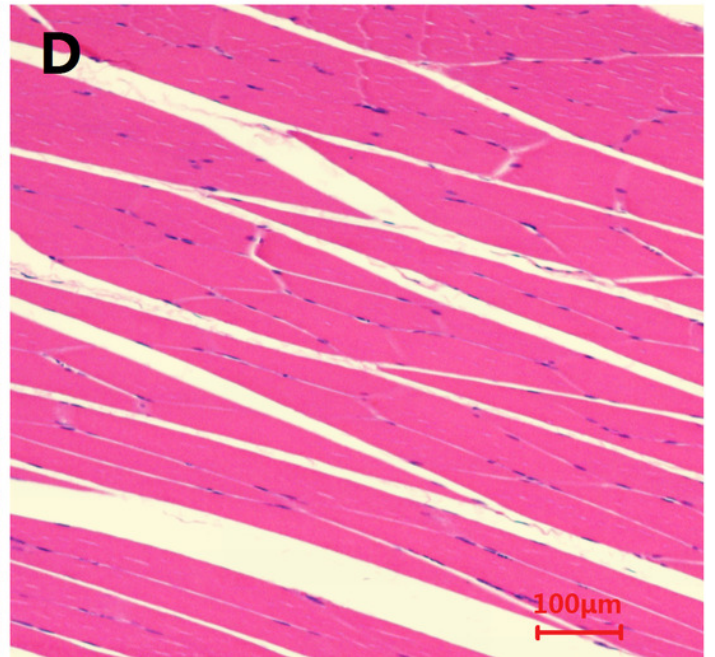
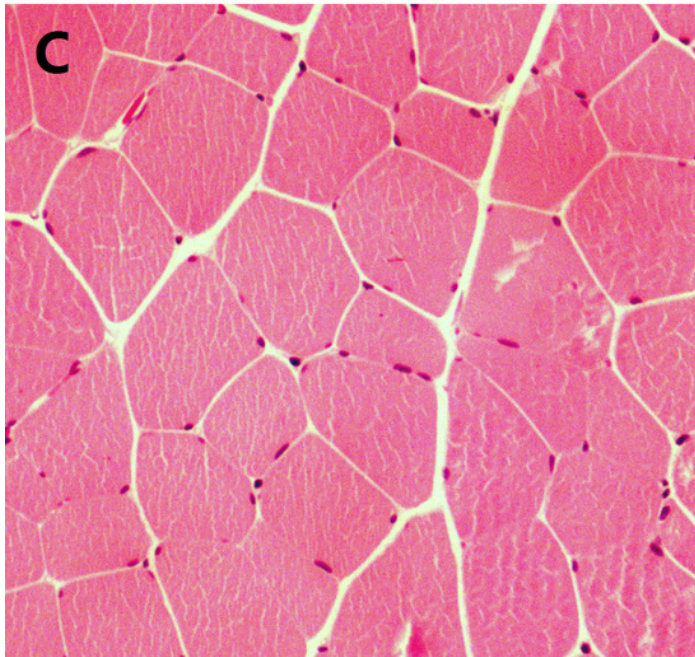
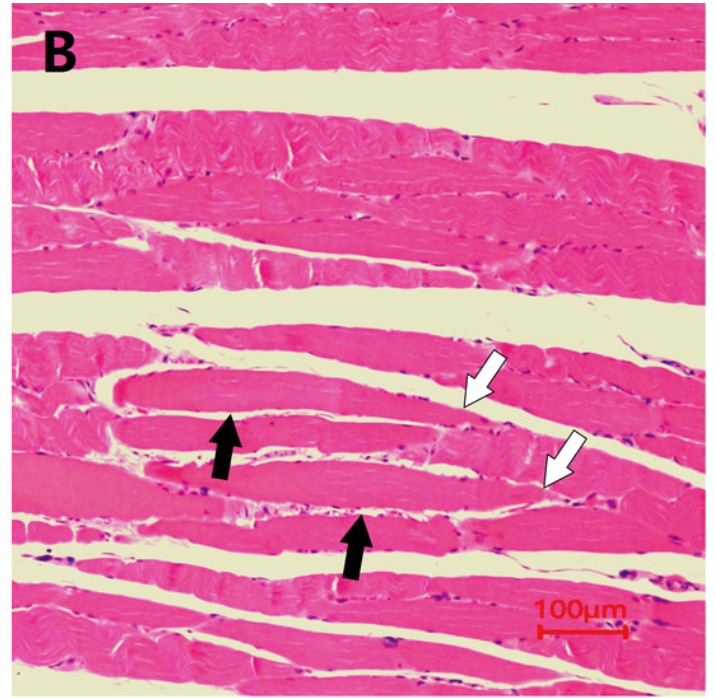
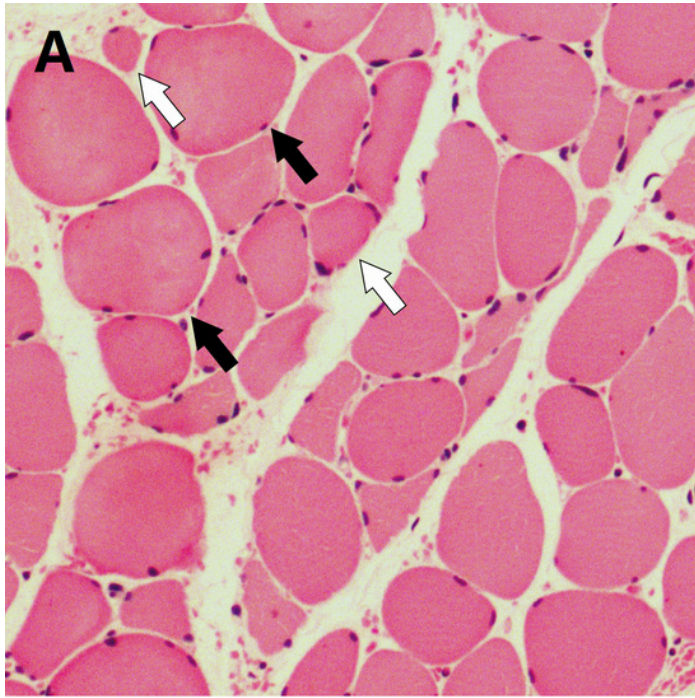


## Figure 5

Comparison of the MVD in rat muscle fibres between the MTrP rats and normal controls.

(A) and (B) Images of IHC staining for CD31 in rats from the control group and the MTrP group, respectively. (C) Comparison of the MVD in muscle fibres from rats in the two groups; \*  $P < 0.001$ .

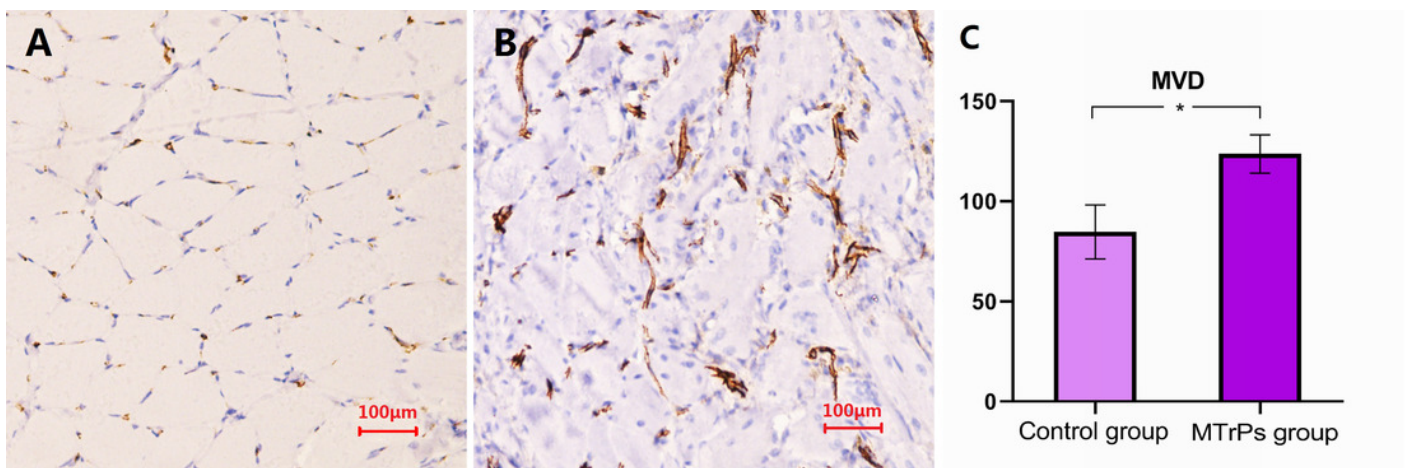


## Figure 6

Expression of HIF-1 $\alpha$  and VEGF in two groups of rats.

\* indicates a significant difference between the MTrPs group and normal control group ( $P < .001$ ).

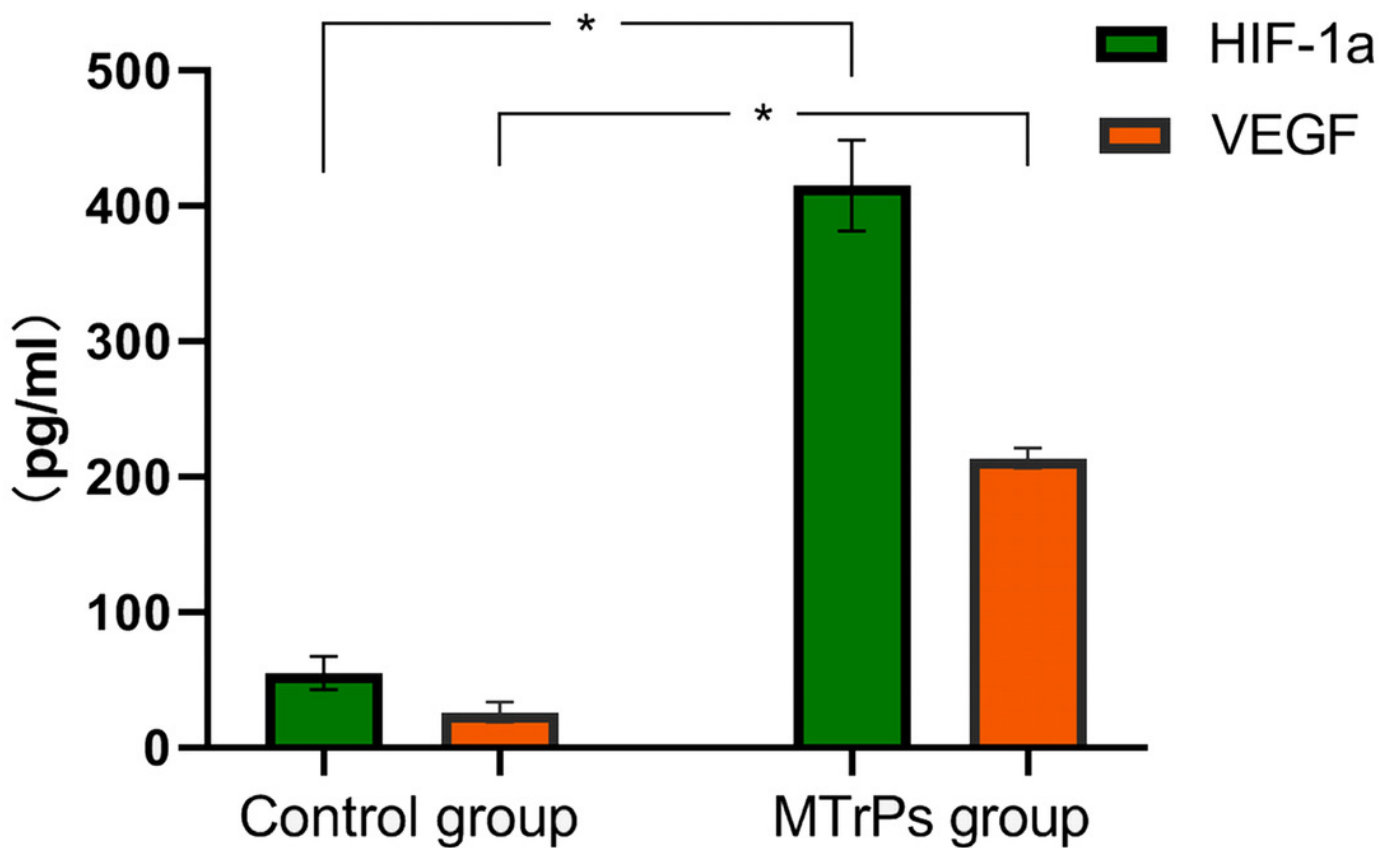


## Figure 7

Linear correlation plots between blood flow signals and HIF-1 $\alpha$  levels, VEGF levels and MVD performed in the active MTrP group.

Linear correlation analysis showed between VEGF levels and blood flow signal grades, MVD and blood flow signal grades a coefficient of correlation ( $r$ )  $> 0.5$  ( $p < 0.05$ ). A significant correlation between HIF-1 $\alpha$  levels and blood flow signal grades was not observed ( $p > 0.05$ ).

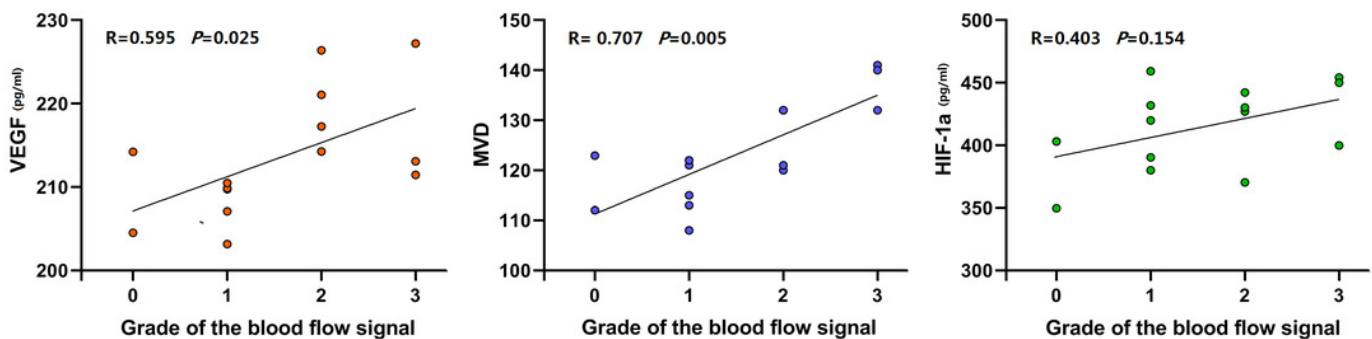


**Table 1** (on next page)

Results of blood flow signal grading.

---

Grade	Criterion	No. (n=14)
0	No blood flow signals	2
I	One or two dot-like blood flow signals	5
II	Three dot-like or a thin- and short-like blood flow signals	4
III	One or more large and longer blood flow signals	3

---